

---

# Thermal-Structural Panel Buckling Tests

---

Randolph C. Thompson and W. Lance Richards

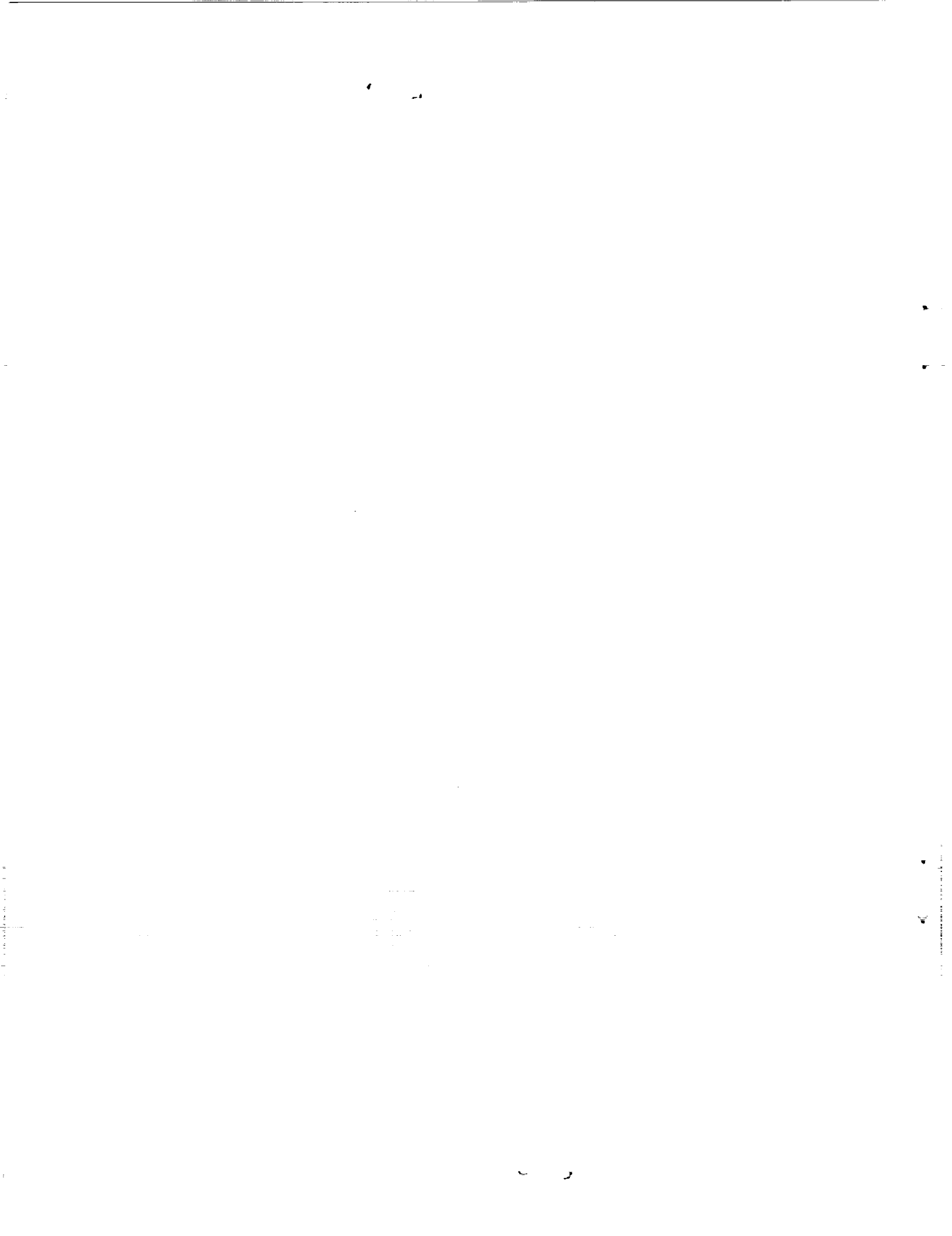
---

(NASA-TM-104243) THERMAL-STRUCTURAL PANEL  
BUCKLING TESTS (NASA) 22 p CSCL 20K

N92-15404

Unclas  
G3/39 0061489

December 1991



---

# Thermal-Structural Panel Buckling Tests

---

Randolph C. Thompson  
PRC Inc., Edwards, California

W. Lance Richards  
NASA Dryden Flight Research Facility, Edwards, California

1991



National Aeronautics and  
Space Administration

**Dryden Flight Research Facility**  
Edwards, California 93523-0273

1

# CONTENTS

|   |    |
|---|----|
| <b>FIGURES</b>                          | iv |
| <b>ABSTRACT</b>                         | 1  |
| <b>NOMENCLATURE</b>                     | 1  |
| <b>INTRODUCTION</b>                     | 1  |
| <b>ACKNOWLEDGEMENTS</b>                 | 2  |
| <b>TEST DESCRIPTION</b>                 | 2  |
| Test Article . . . . .                  | 2  |
| Instrumentation . . . . .               | 3  |
| Data Acquisition and Control . . . . .  | 5  |
| Test Setup . . . . .                    | 5  |
| <b>TEST APPROACH</b>                    | 8  |
| Measurements . . . . .                  | 8  |
| Buckling Prediction Technique . . . . . | 8  |
| Procedures . . . . .                    | 10 |
| <b>RESULTS AND DISCUSSION</b>           | 12 |
| <b>CONCLUDING REMARKS</b>               | 16 |
| <b>REFERENCES</b>                       | 17 |

RECEIVED 1/11/68

# FIGURES

|   |    |
|---|----|
| Figure 1. TMC hat-stiffened panel.  | 3  |
| (a) Skin-side . . . . .   | 3  |
| (b) Hat-side . . . . .  | 3  |
| Figure 2. TMC hat-stiffened panel instrumentation   | 4  |
| (a) Skin-side . . . . .   | 4  |
| (b) Hat-side. . . . .   | 4  |
| Figure 3. 220-kip load frame system. . . . .  | 6  |
| Figure 4. Load platen design . . . . .  | 7  |
| Figure 5. Radiant heating oven design.  | 8  |
| (a) Outer view . . . . .  | 8  |
| (b) Inner view. . . . .   | 8  |
| Figure 6. Single-strain-gage <i>F/S</i> method of predicting local buckling loads.  | 9  |
| (a) Typical strain output as a function of load. . . . .  | 9  |
| (b) Typical <i>F/S</i> plot. . . . .  | 10 |
| Figure 7. Thermal and mechanical loading procedures . . . . .   | 12 |
| Figure 8. Skin-side temperature distribution at 515 °F with panel in the cross-corrugation mode . . . . .                       | 13 |
| Figure 9. Normalized strain distributions at varying cross sections.  | 14 |
| (a) Top cross section . . . . .   | 14 |
| (b) Center cross section . . . . .  | 14 |
| (c) Bottom cross section . . . . .  | 14 |
| Figure 10. Buckling load prediction at an elevated temperature (500 °F) equilibrium condition with the panel in the axial mode. | 15 |
| (a) Typical strain output as a function of load . . . . .   | 15 |
| (b) Typical <i>F/S</i> plot . . . . .   | 16 |

## ABSTRACT

The buckling characteristics of a titanium matrix composite hat-stiffened panel were experimentally examined for various combinations of thermal and mechanical loads. Panel failure was prevented by maintaining the applied loads below real-time critical buckling predictions. The test techniques used to apply the loads, minimize boundary effects, and predict the panel response at high temperatures are presented. Experimentally predicated buckling loads have been shown to compare well with a finite-element buckling analysis for previous panels. Comparisons between test predictions and analysis for this panel are ongoing.

## NOMENCLATURE

|            |                                     |
|------------|-------------------------------------|
| Al         | aluminum                            |
| <i>D</i>   | bending strain, microstrain         |
| DACS       | Data Acquisition and Control System |
| <i>F</i>   | applied compression load, lb        |
| <i>F/S</i> | force/stiffness                     |
| NASP       | National Aero-Space Plane           |
| T          | temperature, °F                     |
| TMC        | titanium matrix composite           |
| V          | vanadium                            |

## INTRODUCTION

Advances in hypersonic vehicle technology have led to the design and fabrication of potential National Aero-Space Plane (NASP) fuselage and wing panel structural subcomponents. A hat-stiffened panel is one subcomponent that has been fabricated into two test articles. The first test article was made from monolithic titanium and the other test article was made from titanium matrix composite (TMC). These panels are designed to carry loads both parallel and perpendicular to the hat stiffeners; therefore, the buckling characteristics are critical to their design. Determining these characteristics under a variety of thermal-mechanical test configurations, while maintaining panel integrity, has required the use of innovative test techniques.

Personnel at the National Aeronautics and Space Administration (NASA) Dryden Flight Research Facility (DFRF), in a cooperative effort with the McDonnell Douglas Corp., have completed a thermal-mechanical test program on a monolithic Ti 6Al-4V hat-stiffened panel. This panel was nondestructively tested to 500 °F to examine its buckling characteristics and to validate analytical tools [1]. The test techniques developed to test the monolithic panel recently have been used to test the TMC panel at 500 and 1200 °F in similar thermal-mechanical loading configurations.

Described in this paper are: (1) the test techniques developed to apply the thermal-mechanical loads and minimize boundary effects and (2) the application of a single-strain-gage force/stiffness (*F/S*)

buckling prediction technique [2] to the TMC panel. The results contained in this paper show typical experimental data and will not cover every test configuration. In some cases the trends of the results and not the magnitudes are presented because of applicable International Traffic in Arms Regulations (ITAR) restrictions.

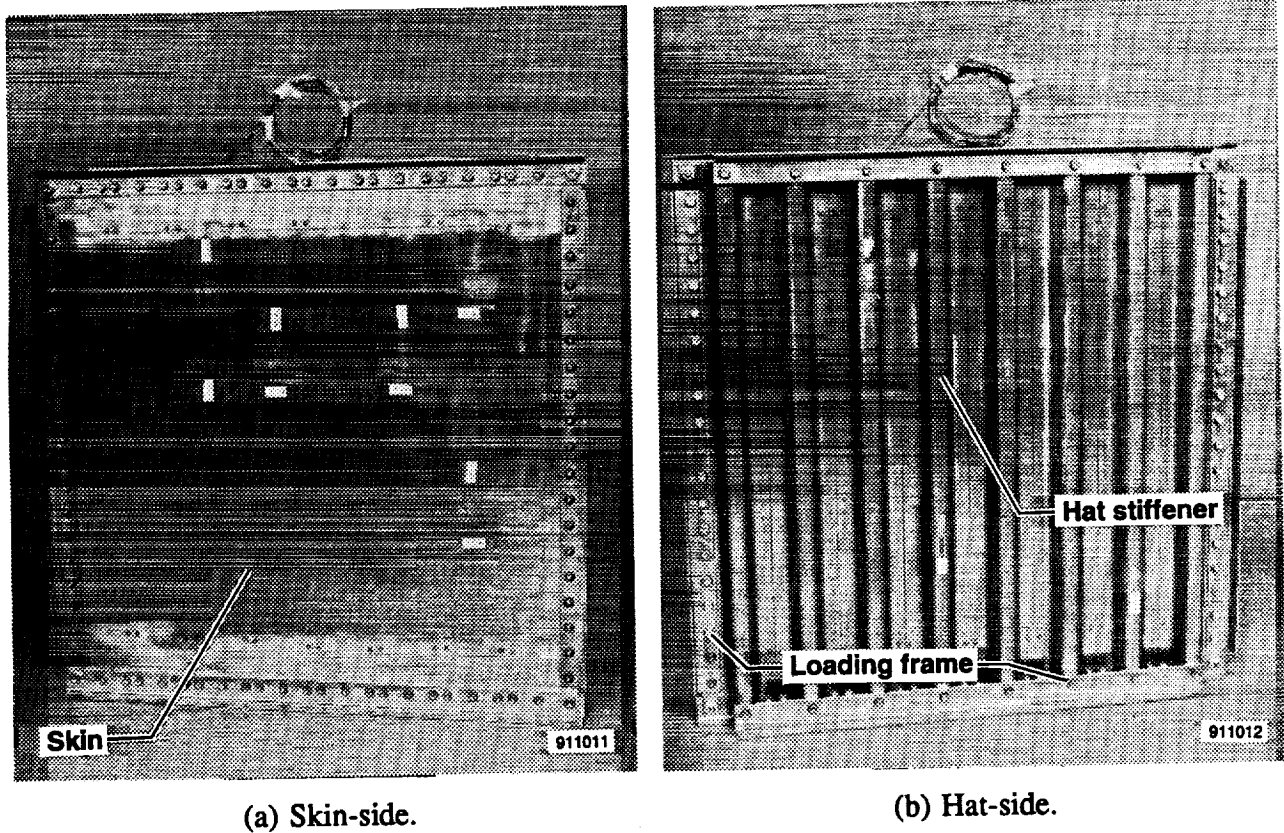
## ACKNOWLEDGEMENTS

The authors would like to acknowledge Roger A. Fields (NASA-DFRF) for his extensive contributions to the development of the single-strain-gage  $F/S$  method and Larry D. Hudson (NASA-DFRF) for his work in apparent strain characterization of high-temperature strain gages used on the TMC panel. The authors would also like to acknowledge the McDonnell Douglas Corp. for providing the test articles and finite-element buckling analysis on this project.

## TEST DESCRIPTION

### Test Article

The test article investigated recently is a TMC hat-stiffened panel representative of a fuselage or wing skin panel of a future hypersonic vehicle (the NASP). The panel measures nominally 24 in. square and 1.25 in. thick (including the height of the hat stiffeners) with eight hat stiffeners attached by spot welds to a flat skin (Fig. 1). L-shaped and T-shaped frames are bolted to all four sides of the panel to produce a load frame. The panel is designed to carry loads parallel (axially) and perpendicular (cross corrugation) to the hat stiffeners and is therefore buckling critical in the axial and cross-corrugation directions.



(a) Skin-side.

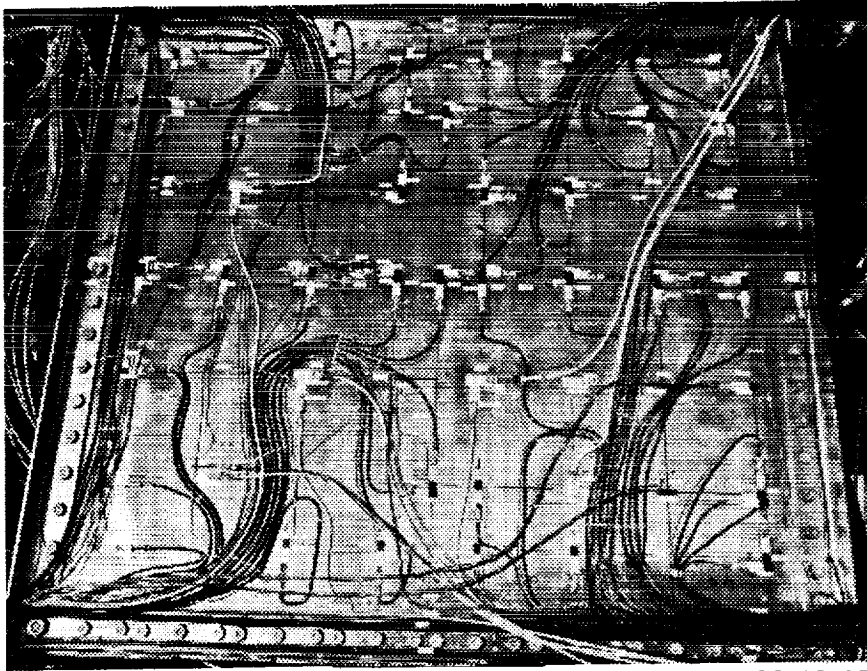
(b) Hat-side.

Figure 1. TMC hat-stiffened panel.

### Instrumentation

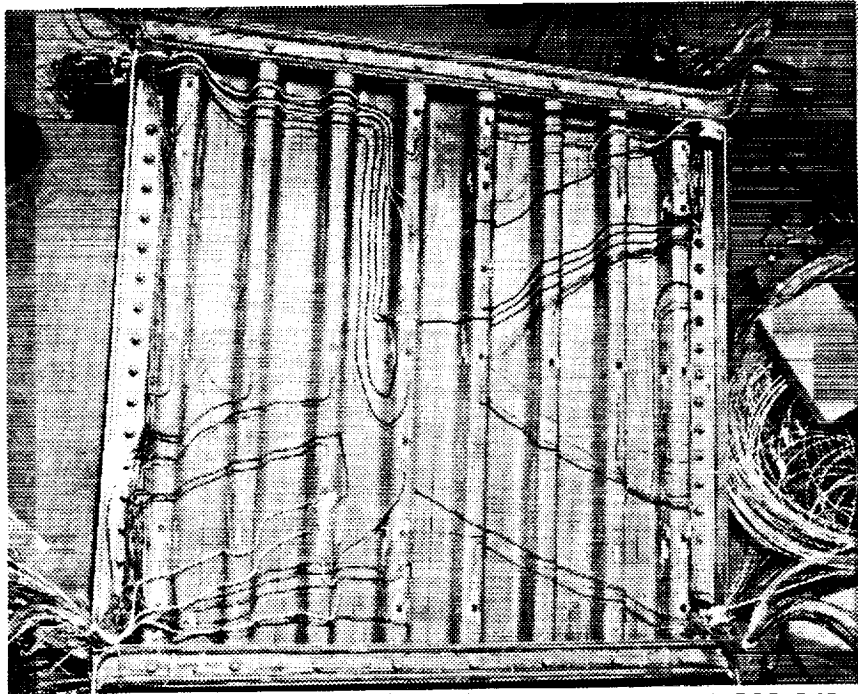
The TMC panel was instrumented extensively with 322 sensors to obtain thorough measurements for validating finite-element buckling models and monitoring real-time panel integrity. The instrumentation included 120 Micro-Measurement (Raleigh, North Carolina) foil strain gages (WK-06-125-AD-350); 14 Micro Engineering II (Upland, California) high-temperature foil strain gages (NZ-2104-120-L); 9 Eaton (El Segundo, California) weldable strain gages (MG425); 3 Battelle (Columbus, Ohio) high-temperature free filament wire strain gages (BCL-3); 164 Inconel<sup>®</sup> sheathed type K (Chromel-Alumel, Hoskins Manufacturing Co., Hamburg, Michigan) thermocouples, and 12 deflection potentiometers. Figure 2(a) shows instrumentation on the skin-side of the panel. Strain gages were positioned in the axial and cross-corrugation directions and were distributed over the panel to provide an overall understanding of the panel behavior. The deflection potentiometer attachment points were evenly distributed on the skin-side of the panel between hat-stiffener legs to measure out-of-plane deformations. The potentiometers were attached to the panel through holes in the high-temperature oven by quartz glass rods to minimize thermal expansion errors. Figure 2(b) is a photograph of the hat-stiffened side of the panel. Strain gages were positioned in-line with the hats and were located on the cap and legs of the hat stiffeners. Thermocouples were distributed on both sides of the panel and on the loading frames to measure panel temperatures. To promote uniform temperature distributions the panel was painted with high-emissivity paint capable of withstanding the elevated test temperatures.

<sup>®</sup> Inconel is a registered trademark of Huntington Alloy Products Division, International Nickel Co., Huntington, West Virginia.



EC90 12-18

(a) Skin-side.



EC89 342-1

(b) Hat-side.

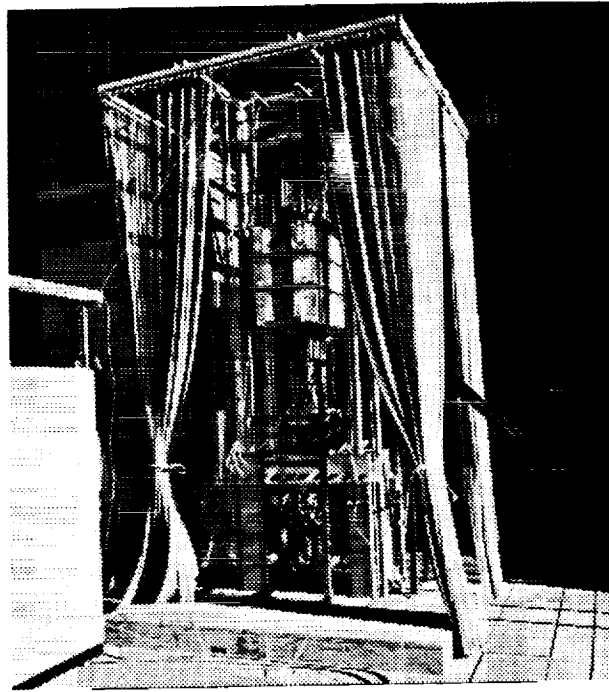
Figure 2. TMC hat-stiffened panel instrumentation.

## Data Acquisition and Control

Data acquisition and adaptive thermal control were accomplished by using the Data Acquisition and Control System (DACS) at the NASA DFRF Thermostructures Research Facility [3]. The primary function of the DACS is to conduct real-time thermal and mechanical simulation of flight environments on test articles and aircraft. The system is capable of recording 1280 channels of data which includes up to 512 thermal closed-loop and 64 mechanical open-loop control channels. The DACS controls temperature and power level. Temperature can be controlled in the  $-320$  to  $2500$  °F range, with research ongoing to control to  $3000$  °F. The maximum DACS firing level is 3600 quartz lamp pulses each minute, with total available power of 20 MW. The system also provides real-time visual data analysis displays such as  $x-y$  plots, thermal control deviation displays, alphanumeric displays, and single- and dual-strain-gage  $F/S$  displays. The DACS maximum allowable system measurement error is  $\pm 0.15$  percent of reading or  $\pm 20$   $\mu\text{V}$ , whichever is greater. Therefore, for a  $\pm 20$   $\mu\text{V}$  strain measurement input from a single active arm strain gage with a 4-V direct current (DC) excitation voltage, the error band is  $\pm 8$   $\mu\text{in/in}$ . However, this error is reduced with additional active arms and higher excitation voltages. Similarly, a type K thermocouple measurement error with a  $\pm 20$   $\mu\text{V}$  input is equivalent to  $\pm 0.9$  °F.

## Test Setup

Compressive loads were applied to the panel in a 220-kip uniaxial load frame system (Fig. 3). This system consists of a lower hydraulic loading ram and load platen, an upper movable ram and platen that is locked into position while load is applied, and a chain-mail screen to prevent injury in the event of test article failure. A 220-kip load cell was placed between the upper ram and platen and was thermally insulated from the oven to reduce the risk of any temperature-induced errors. Open-loop mechanical control was provided by a digital function generator manned by test support personnel. The load cell has a precision of 0.1 percent of reading while the DACS has a precision of  $\pm 1$  count or approximately  $\pm 50$  lb. Therefore a load cell reading of 50,000 lb is precise to  $\pm 100$  lb.



EC89 38-1

Figure 3. 220-kip load frame system.

The test setup was designed to maintain uniform temperatures on the panel during the application of compressive mechanical loads. Controlling the panel boundary temperature was essential to produce realistic and uniform flight loads and simplify the finite-element analysis of the panel. Satisfying these requirements was difficult because of the significant interaction between the thermal and mechanical loads. If conventional load frame hardware were used to apply compressive loads the massive load platens would create heat sinks at the panel boundaries. Likewise, heat conduction to the load platen would cause the platen to warp and introduce nonuniform mechanical loads into the panel. Therefore, a system of heated and cooled platens (Fig. 4) was used to apply uniform thermal and mechanical loads simultaneously. The platen shown supporting the vertically positioned panel was internally heated with 13 cartridge heaters spaced 2 in. apart and oriented perpendicular to the prominent axis of the platen. Power to the cartridge heaters was controlled manually by a power control unit to achieve the desired platen temperature time history. The 1-in.-thick heated platen was fabricated from Ti 6Al-4V to avoid inducing thermal stresses in the panel caused by differences in the coefficients of thermal expansion between the panel and platens. Insulated water-cooled platens maintained at room temperature were used to prevent heat conduction to the testing machine and load cell. A 0.25-in.-thick layer of semirigid insulation was placed between the heated platen and the 3-in.-thick water-cooled steel platen. The water manifolds shown in this figure were used to route water through 13 coolant passages in the cooled platen.

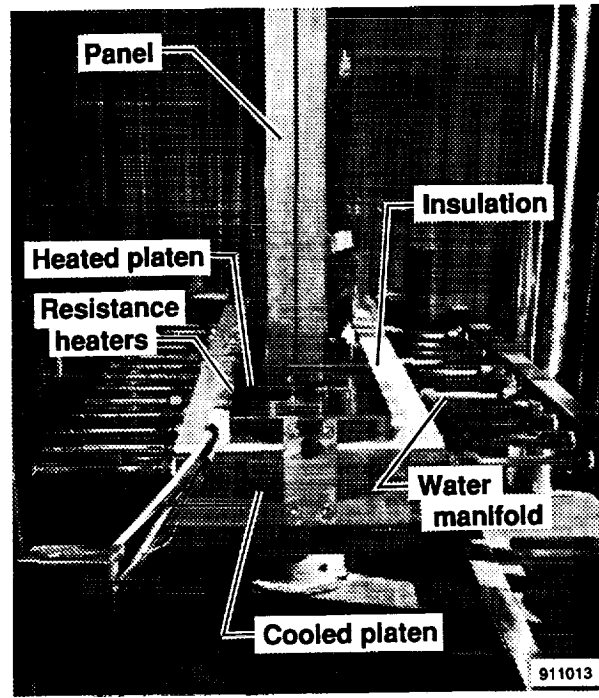
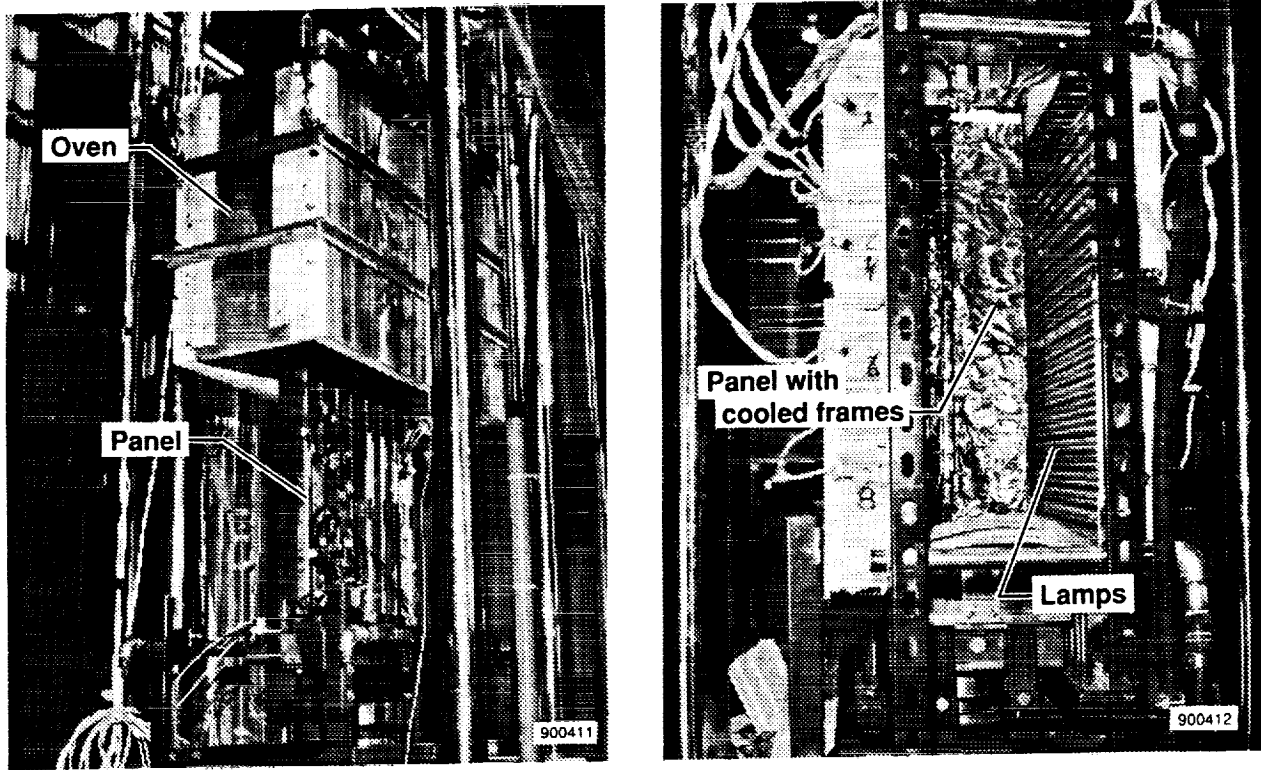


Figure 4. Load platen design.

The ceramic box oven shown in Fig. 5(a) was used to heat the panel to 500 and 1200 °F. The oven consists of a 0.125-in.-thick aluminum sheet box lined with 1.5-in.-thick ceramic block insulation attached with high-temperature adhesive. Forty-eight quartz lamps (24 on each side) were spaced 1-in. apart and aligned horizontally on both sides of the oven (Fig. 5(b)). The 41.8-in.-long lamps extended approximately 6 in. past each side of the panel to provide a more uniform heat flux across the panel. The 48 quartz lamps were divided into 8 independent thermal closed-loop control zones (4 on each side). Thermocouples located on both sides of the panel were used as feedback to adaptively adjust the lamp power to achieve the desired heating rate. Ceramic fences (not shown) were placed between each of the control zones to minimize heat convection losses from the top of the oven. The oven was suspended from the load frame upper movable ram to permit easy access to the panel and instrumentation before and after testing. Figure 5(b) shows the oven lowered into position around the panel and also shows the potentiometer quartz rods attached to the panel to make out-of-plane deflection measurements.

ORIGINAL PAGE  
BLACK AND WHITE PHOTOGRAPH



(a) Outer view.

(b) Inner view.

Figure 5. Radiant heating oven design.

## TEST APPROACH

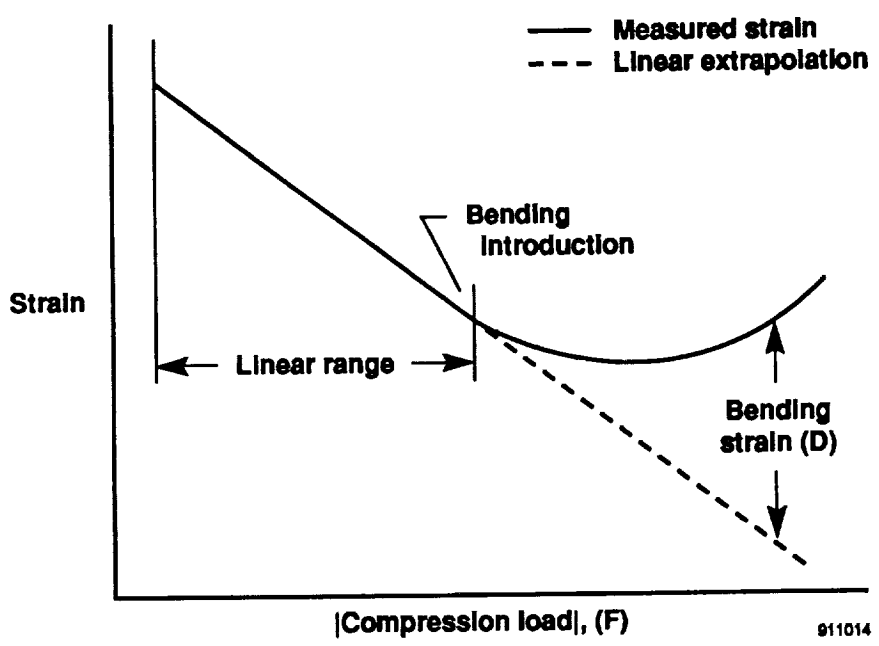
### Measurements

Temperature, out-of-plane deflection, and strain measurements were made on the TMC panel using the instrumentation described previously. Thermocouple and deflection potentiometer measurements are adequately standardized for the environment applied to the TMC panel. However, strain gages that are used at elevated temperatures must be characterized for thermal output or apparent strain. Apparent strain characteristics are different for each type of strain gage and therefore require different apparent strain test techniques for each type of gage: bonded foil, high-temperature foil, high-temperature wire, or weldable. Apparent strain test techniques for each of these types of strain gages are discussed in Ref. [4].

### Buckling Prediction Technique

A single-strain-gage  $F/S$  technique, an adaptation of the  $F/S$  technique developed by Jones and Green [5], was used to predict panel buckling loads [1]. This method was necessary because instrumenting the hat-stiffened panels with back-to-back strain gages would have to occur before fabrication. Since the back-to-back strain gages could not survive the fabrication process a single strain gage was used to determine the local bending strain. The single-strain-gage method divides the gage output into

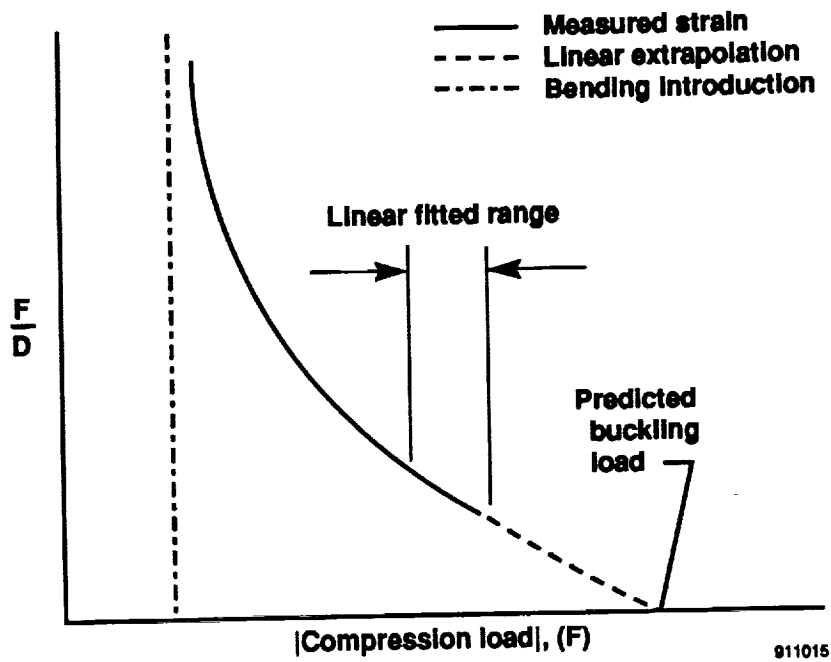
two parts: a linear and nonlinear response. Figure 6(a) shows the typical response of a strain gage to load under uniaxial compression in a buckling situation. The gage responds linearly up to a load where bending is introduced, after that point it responds nonlinearly. The single-strain-gage method uses the linear response of the gage to determine the bending strain during the nonlinear response portion. By fitting a straight line through the linear portion, an extrapolation beyond the bending introduction point can be made. The assumption is that if the gage would continue to respond linearly with load, the output of the gage would follow the dashed line. The extrapolation beyond the bending introduction point enables the bending strain to be computed as the difference between the measured strain and the strain from the linear extrapolation. The bending strain can then be used in the  $F/S$  plot.



(a) Typical strain output as a function of load.

Figure 6. Single-strain-gage  $F/S$  method of predicting local buckling loads.

Figure 6(b) is a typical  $F/S$  plot in which  $F/D$  is plotted as a function of  $F$  where  $F$  represents the compressive load and  $D$  the bending strain found in Fig. 6(a). The curve moves downward to the right as the critical buckling load is approached. By selecting a linear-fitted range near the bottom portion of the  $F/S$  curve, a line can be extrapolated down to the load axis to predict the buckling failure load. The fitted range is usually the lower portion of the  $F/S$  curve and is based upon judgement, experience, and upon the assumption that no load path or mode changes will occur before the intersection. In this paper, the prediction is of the first mode elastic buckling load, which is considered the critical buckling load.



(b) Typical  $F/S$  plot.

Figure 6. Concluded.

A real-time single-strain-gage  $F/S$  evaluation was conducted to examine the TMC panel integrity during thermal-mechanical testing. Software was developed on the DACS and on Sun SPARCstations (Sun Microsystems Inc., Mountain View, California) for a real-time display of the  $F/S$  method. An iterative incremental load application procedure utilizing the single-strain-gage method was developed. This procedure allows the panel to be tested close to critical buckling loads.

### Procedures

The TMC panel was subjected to a series of nondestructive combined thermal equilibrium and mechanical loads. First, the panel was mechanically loaded at room temperature and at elevated equilibrium temperatures in the cross-corrugation mode with and without water-cooled frames. These water-cooled frames were used to apply an in-plane thermal gradient across the panel. Next, the panel was mechanically loaded at room temperature and at elevated equilibrium temperatures in the axial mode. The panel was also held at constant loads in the cross-corrugation mode while an elevated equilibrium temperature profile was applied. An extensive test matrix was followed to provide test data for a variety of test configurations.

Load alignment was considered critical to prevent eccentric loading and to create a uniform load distribution. Alignment was monitored in real time by checking strain gage outputs on skin-side cross sections near the top, bottom, and center of the panel. Load alignment was then optimized by securing the panel in guides attached to the platens and by shimming the top and bottom edges of the panel.

Thermal and mechanical load profiles were applied to the panel using the DACS for closed-loop oven control and manual control for the heated platens and load frame. Figure 7 shows a schematic of the thermal-mechanical loading procedure for an elevated temperature test. First, the panel was seated by applying a mechanical preload (1). Then the platen heating was started before the oven heating because of the platen mass and inherent thermal inertia (2). When the temperature of the heated platens reached 30 to 40 °F above the panel temperature the closed-loop temperature control on the panel was started (3). The panel and platens were then held at constant temperatures at 100 °F increments for several minutes to obtain uniform panel temperatures (4). Once the panel and platens reached a uniform equilibrium temperature of 500 °F the mechanical loading began (5). Load was applied in small increments to obtain a linear range for the single-strain-gage  $F/S$  method (6). Load was then held constant to allow time to enact the real-time single-strain-gage  $F/S$  software (7). Finally, loading continued until it was determined from the real-time single-strain-gage  $F/S$  plots to be the maximum possible load while maintaining panel integrity (8).

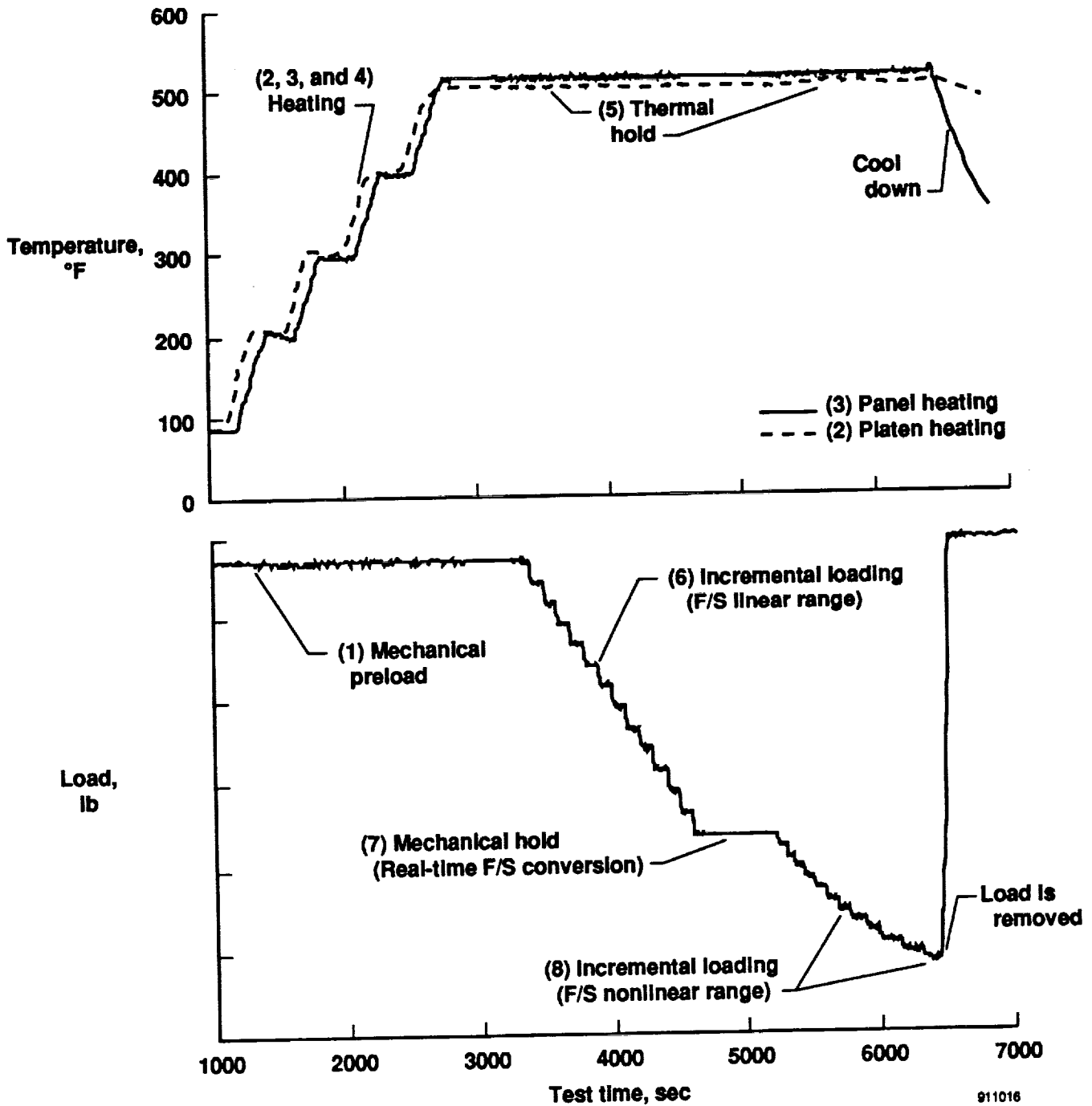


Figure 7. Thermal and mechanical loading procedures.

## RESULTS AND DISCUSSION

Experience with testing the Ti 6Al-4V monolithic panel has shown that the most detailed of the finite-element models used to analyze the panel will not provide good correlation between measured and predicted strains unless the temperature field is defined accurately [1]. Therefore, of particular interest in these tests, as in all elevated-temperature structural testing, is well-defined temperature distributions.

Figure 8 shows a combined surface and contour plot of a temperature distribution at 515 °F over the skin-side of the TMC panel oriented with load applied perpendicular (cross corrugation) to the hat stiffeners. The deviation from a uniform temperature distribution of 515 °F is +5 to -60 °F with the bottom corners of the panel exhibiting the largest deviation.

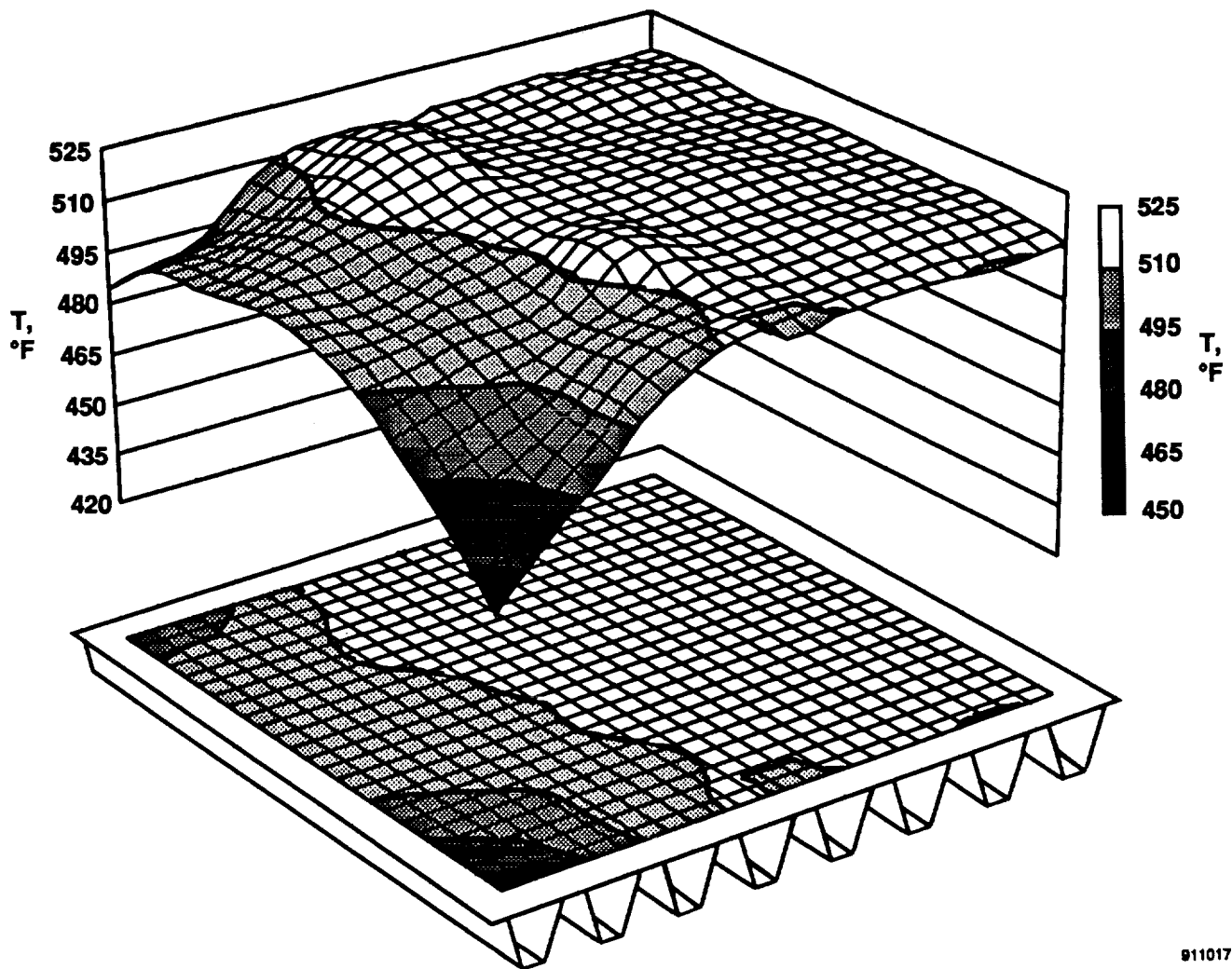
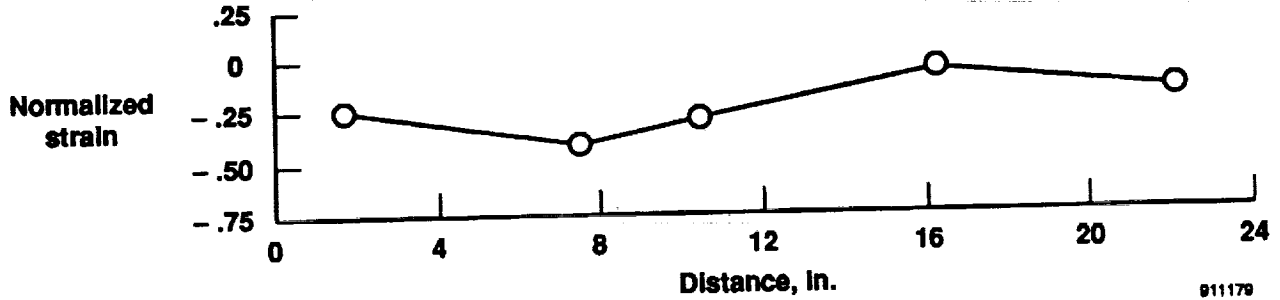


Figure 8. Skin-side temperature distribution at 515 °F with panel in the cross-corrugation mode.

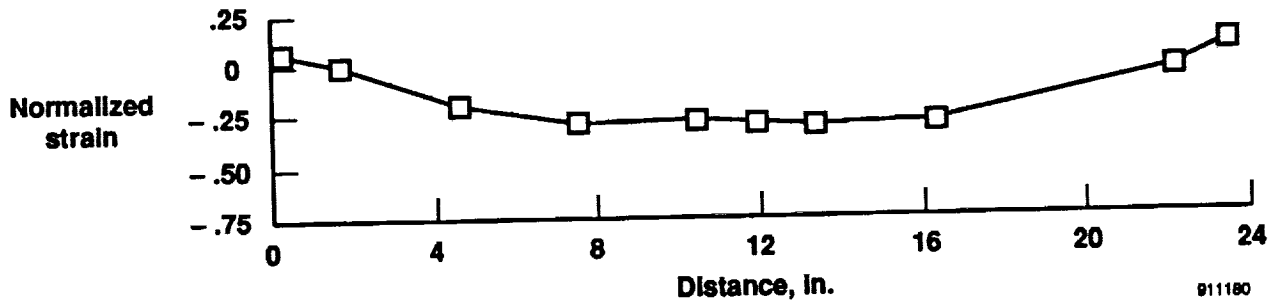
Two of the test requirements for the TMC panel were to load the panel in the axial and cross-corrugation directions and to obtain thorough temperature and strain measurements. These requirements led to a large amount of instrumentation wiring that needed to be routed off the panel in the corners. Thermal shading of the panel will occur when large bundles of instrumentation wires are routed off a test article at any one point. In addition, convection losses can occur at the oven corners where the instrumentation wires exit the oven. From Fig. 8 it is evident that convection losses and thermal shading play a large part in affecting the overall panel temperature distribution.

Load alignment was monitored by checking strain gage outputs on skin-side cross sections near the top, bottom, and center of the panel (Fig. 9). These strain distributions are on the skin-side of the panel

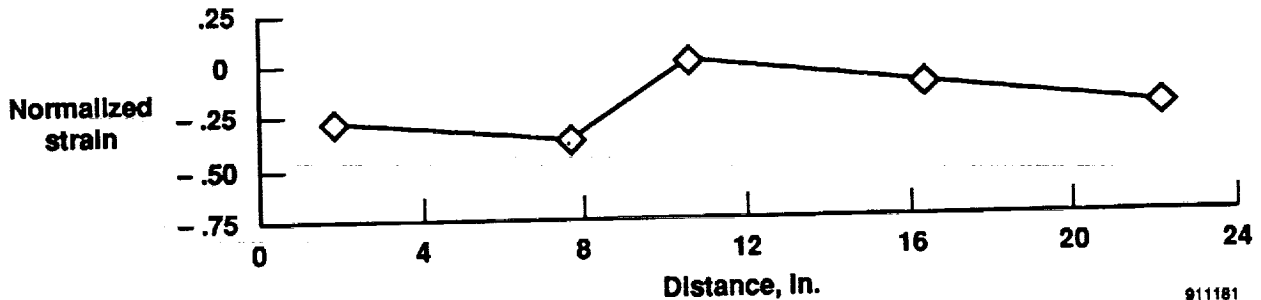
for an elevated temperature (500 °F) test with load applied parallel (axially) to the hat stiffeners. The strain magnitudes are shown normalized with respect to the absolute value of the largest strain value on the skin-side of the panel. Figures 9(a) and (c), the top and bottom of the panel, show a noticeably nonuniform strain distribution. These higher strain levels are a result of some of the bolts in the frames starting to carry load before others. Also, uneven load introduction can occur because the frames are not parallel or rigid. A more uniform strain distribution is seen at the center cross section of the panel (Fig. 9(b)). The center panel strain distribution is not ideally uniform because the axially positioned frames carry some of the load at the panel edges. However, the center of the panel was not significantly affected by any nonuniform load introduced into the panel edges.



(a) Top cross section.



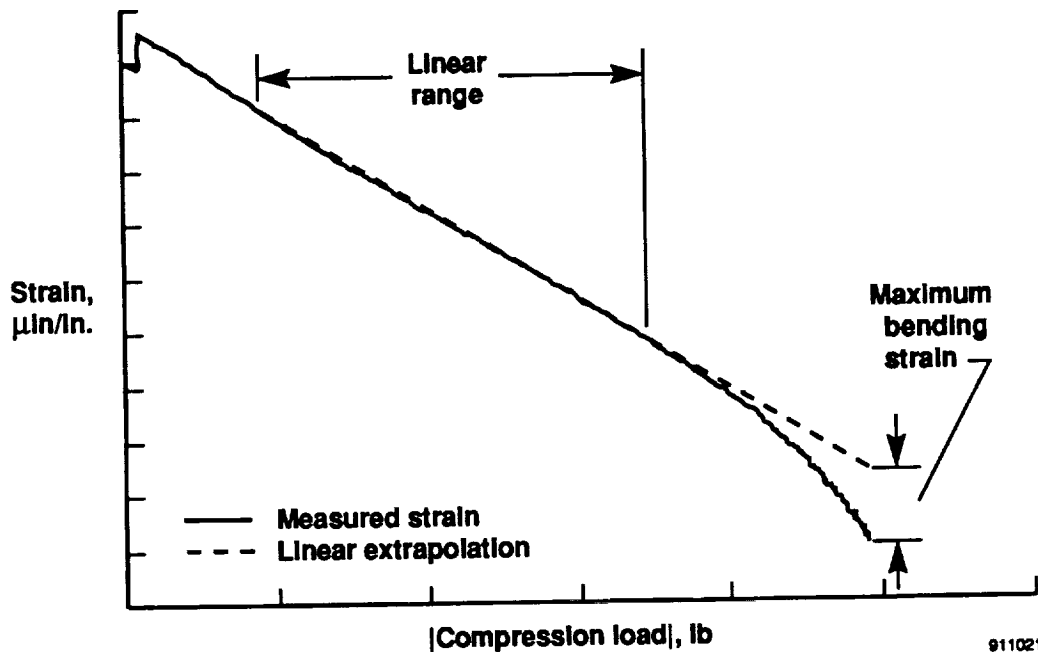
(b) Center cross section.



(c) Bottom cross section.

Figure 9. Normalized strain distributions at varying cross sections.

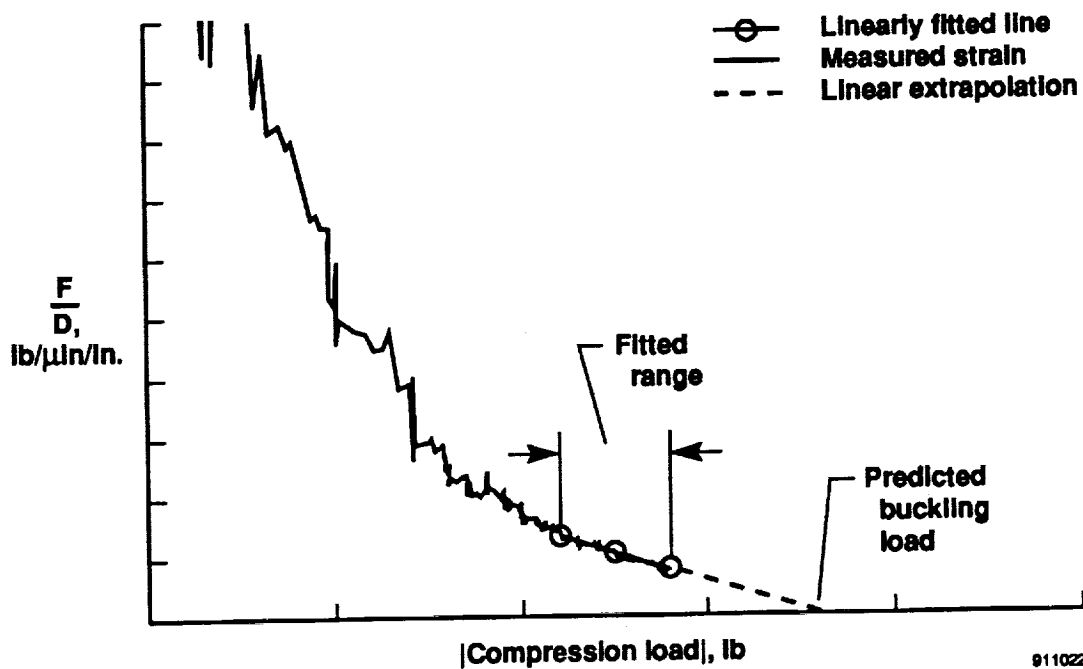
Single-strain-gage  $F/S$  buckling load predictions were made at room temperature and at elevated temperature equilibrium conditions. Figure 10(a) is a typical plot of strain as a function of load for the case of axial loading at a steady-state equilibrium condition of 500 °F. The gage used for the plot is located on the skin-side near the center of the panel and between the legs of a hat stiffener. The gage response is nearly linear up to a certain load, after which bending is introduced and the gage responds nonlinearly. The bending strain is determined by the difference between the extrapolation of a linear fit through the linear range and the measured strain beyond the bending introduction point.



(a) Typical strain output as a function of load.

Figure 10. Buckling load prediction at an elevated temperature (500 °F) equilibrium condition with the panel in the axial mode.

The bending strain is then used in the single-strain-gage  $F/S$  plot shown in Fig. 10(b). This plot shows  $F/D$  plotted as a function of  $F$ , where  $D$  is the calculated bending strain of Fig. 10(a). The lower limit of  $F/D$  values is reached as a result of experience gained from previous tests. The desire is to get the  $F/D$  value as low as possible without buckling the panel to achieve a good prediction of the critical buckling load. To obtain an accurate approximation of the critical buckling load, a fitted range of the  $F/S$  curve needs to be selected. For this case a straight line was drawn through the fitted range and the critical buckling load was predicted. Figure 10(b) does not provide the exact local buckling load but this local prediction does provide an estimate of the general instability occurring in the panel. A good estimate of the overall panel buckling load can be obtained by averaging local buckling load predictions over an area of the panel away from the edges. The single-strain-gage method provides a good understanding of the local behavior of the panel (load path and mode changes can be readily observed) and is used to make real-time judgements of panel integrity [2].



(b) Typical  $F/S$  plot.

Figure 10. Concluded.

Comparisons between test predictions and a finite-element buckling analysis performed by personnel at the McDonnell Douglas Corp. are ongoing for the TMC panel. However, single-strain-gage  $F/S$  predictions have been shown to correlate to within 10 percent of analysis for the thermal-mechanical buckling tests performed on the Ti 6Al-4V monolithic hat-stiffened panel [2].

## CONCLUDING REMARKS

A titanium matrix composite (TMC) hat-stiffened panel has been subjected to a series of nondestructive combined thermal equilibrium and mechanical loads to examine its buckling characteristics. Test techniques were used to test the panel to 500 and 1200 °F. Mechanical loads were applied to the panel using a 220-kip load frame system. Load alignment was optimized by shimming the top and bottom of the panel. Alignment was monitored in real time by checking strain gage outputs on skin-side cross sections near the top, bottom, and center of the panel. The center of the panel away from the edges was minimally affected by any nonuniform load introduction. A combined heated and cooled platen was designed to prevent warping of the upper and lower loading platens and to provide a near-uniform temperature distribution at the panel edges. High test temperatures were obtained by using quartz lamp radiant heating arranged in a ceramic box oven enclosing the panel. Deviations from a uniform temperature distribution occurred because of convection losses at the oven corners and thermal shading from instrumentation wires. A single-strain-gage force/stiffness method was used to predict panel buckling loads. These predictions have been shown to correlate well with analysis for a monolithic titanium panel which was tested in similar thermal-mechanical loading configurations as the TMC panel. For the TMC hat-stiffened panel, comparisons between test predictions and a finite-element buckling analysis are ongoing.

## REFERENCES

1. Percy, Wendy C., and Fields, Roger A., "Buckling Analysis and Test Correlation of Hat Stiffened Panels for Hypersonic Vehicles," AIAA-90-5219, Oct. 1990.
2. Hudson, Larry D., and Thompson, Randolph C., *Single-Strain-Gage Force/Stiffness Buckling Prediction Techniques on a Hat-Stiffened Panel*, NASA TM-101733, 1991.
3. Zamanzadeh, Behzad, Trover, William F., and Anderson, Karl F., "DACCS II - A Distributed Thermal/Mechanical Loads Data Acquisition and Control System," *Proceedings of the International Telemetry Conference, San Diego, CA, Oct. 26-29, 1987*, 1987, pp. 737-752.
4. Hudson, Larry D., and Thompson, Randolph C., "High Temperature Test Techniques and Instrumentation on a Hat-Stiffened Panel," *Ninth National Aero-Space Plane Technology Symposium Vol. VI-Structures*, NASP CP-9057, paper no. 158, 1990.
5. Jones, Robert E., and Greene, Bruce E., "The Force/Stiffness Technique for Nondestructive Buckling Testing," AIAA-74-351, Apr. 1974.

# REPORT DOCUMENTATION PAGE

Form Approved  
OMB No. 0704-0188

Public reporting burden for this collection of information is estimated to average 1 hour per response, including the time for reviewing instructions, searching existing data sources, gathering and maintaining the data needed, and completing and reviewing the collection of information. Send comments regarding this burden estimate or any other aspect of this collection of information, including suggestions for reducing this burden, to Washington Headquarters Services, Directorate for Information Operations and Reports, 1215 Jefferson Davis Highway, Suite 1204, Arlington, VA 22202-4302, and to the Office of Management and Budget, Paperwork Reduction Project (0704-0188), Washington, DC 20503.

|  |   |   |                                   |
|--|---|---|-----------------------------------|
| <b>1. AGENCY USE ONLY (Leave blank)</b>  | <b>2. REPORT DATE</b><br>December 1991                          | <b>3. REPORT TYPE AND DATES COVERED</b><br>Technical Memorandum             |                                   |
| <b>4. TITLE AND SUBTITLE</b><br><br>Thermal-Structural Panel Buckling Tests  |   | <b>5. FUNDING NUMBERS</b><br><br>WU-505-63-40                               |                                   |
| <b>6. AUTHOR(S)</b><br>Randolph C. Thompson (PRC Inc., Edwards, California)<br>W. Lance Richards (Dryden Flight Research Facility, Edwards, California)  |   |   |                                   |
| <b>7. PERFORMING ORGANIZATION NAME(S) AND ADDRESS(ES)</b><br>Dryden Flight Research Facility<br>P.O. Box 273<br>Edwards, California 93523-0273   |   | <b>8. PERFORMING ORGANIZATION REPORT NUMBER</b><br><br>H-1778               |                                   |
| <b>9. SPONSORING/MONITORING AGENCY NAME(S) AND ADDRESS(ES)</b><br>National Aeronautics and Space Administration<br>Washington, DC 20546-0001   |   | <b>10. SPONSORING/MONITORING AGENCY REPORT NUMBER</b><br><br>NASA TM-104243 |                                   |
| <b>11. SUPPLEMENTARY NOTES</b><br>Prepared for presentation at the Society for Experimental Mechanics 1991 Fall Conference on "Structural Testing Technology at High Temperature," Dayton, Ohio, November 4-6, 1991.   |   |   |                                   |
| <b>12a. DISTRIBUTION/AVAILABILITY STATEMENT</b><br><br>Unclassified — Unlimited<br>Subject Category 39   |   | <b>12b. DISTRIBUTION CODE</b>   |                                   |
| <b>13. ABSTRACT (Maximum 200 words)</b><br><br>The buckling characteristics of a titanium matrix composite hat-stiffened panel were experimentally examined for various combinations of thermal and mechanical loads. Panel failure was prevented by maintaining the applied loads below real-time critical buckling predictions. The test techniques used to apply the loads, minimize boundary effects, and predict the panel response at high temperatures are presented. Experimentally predicated buckling loads have been shown to compare well with a finite-element buckling analysis for previous panels. Comparisons between test predictions and analysis for this panel are ongoing. |   |   |                                   |
| <b>14. SUBJECT TERMS</b><br>Buckling; Elevated temperatures; Force/stiffness; Hat-stiffened panel; Hypersonic vehicle; Metal matrix composite; Strain gages; Test techniques   |   | <b>15. NUMBER OF PAGES</b><br>22  |                                   |
|  |   | <b>16. PRICE CODE</b><br>A02  |                                   |
| <b>17. SECURITY CLASSIFICATION OF REPORT</b><br>Unclassified   | <b>18. SECURITY CLASSIFICATION OF THIS PAGE</b><br>Unclassified | <b>19. SECURITY CLASSIFICATION OF ABSTRACT</b>                              | <b>20. LIMITATION OF ABSTRACT</b> |